Check for updates

ce/papers Proceedings in civil engineering

eurosteel CRACOW 2026

WILEY

Full paper

Explainable Boosting Machines for Web-Crippling Resistance Prediction of Cold-Formed Sigma Sections under End-Two-Flange Loading

Lenganji Simwanda[1], Thushanthan Kannan[2], Kajaharan Thirunavukkarasu[2], Mohamed Sifan[3], Keerthan Poologanathan[2], Kajeenthan Kamalaseelan[4], Jeyasutha Lingaretnam[5], Sunday Popo-Ola[6]

Correspondence

Lenganji Simwanda
Klokner Institute, Czech Technical University in Prague
Šolínova 7, 166 08 Prague 6, Czech Republic
Email: lenganji.simwanda@cvut.cz

[1] Klokner Institute, Czech Technical University in Prague.
[2] Faculty of Engineering and Environment, Northumbria University, Newcastle upon Tyne, UK
[3] School of Engineering, University of Surrey, Guilford, UK
[4] Department of Civil Engineering, British College of Applied Studies, Sri Lanka.
[5] Department of Civil Engineering, University of Moratuwa, Sri Lanka
[6] Department of Civil and Environmental Engineering, Imperial College London, UK

Abstract

Cold-formed steel (CFS) sigma sections are highly efficient but vulnerable to web crippling under concentrated bearing loads. Current design provisions in AISI S100, AS/NZS 4600 and EN 1993-1-3 are largely calibrated for channel and Z-sections and often give conservative or scattered predictions for sigma sections under end–two–flange (ETF) loading. This study presents an explainable machine-learning framework for predicting ETF web-crippling resistance of sigma sections. A validated nonlinear finite-element study in ABAQUS produced 756 simulations covering variations in geometry, yield strength and bearing conditions. Finite-element predictions were verified against experimental data for carbon steel, stainless steel and aluminium, showing mean Test/FE ratios of 0.95–1.01 and coefficients of variation below 5%. Six ensemble models were trained using Bayesian optimisation, with boosting-based methods achieving the best accuracy ($R^2 \approx 1.0$; RMSE < 0.1 kN) and outperforming code equations. SHAP analysis identified thickness, yield strength and bearing length as dominant predictors. The proposed models provide fast, accurate and transparent tools for ETF web-crippling resistance estimation.

Keywords

cold-formed steel, sigma sections, web crippling, ensemble learning, SHAP, ETF loading

1 Introduction

Web crippling is a localised bearing failure that often governs thin-walled cold-formed steel (CFS) members at supports and concentrated load points [1–3]. Sigma sections, characterised by web insets and intermediate stiffeners, are increasingly used because they provide high strength-to-weight efficiency; however, their end–two–flange (ETF) web-bearing response is not well represented in the calibration envelopes of common design equations. Consequently, provisions in AISI S100 / AS-NZS 4600 and EN 1993-1-3 may exhibit bias and dispersion when applied to sigma geometries, particularly across mixed materials and stiffener configurations [1–3, 9–11].

Although recent numerical and design-oriented studies have advanced the understanding of sigma-section web crippling under ETF loading, three limitations remain for practical design: (i) most available equations and code provisions are calibrated mainly on channels/Z-sections and do not generalise reliably to sigma sections with intermediate stiffeners; (ii) existing predictors rarely provide a unified, high-accuracy model that is valid across multiple material families (carbon steel, stainless steel and aluminium) within a single framework; and (iii) explainable machine-learning approaches for sigma sections under ETF loading remain limited, and are seldom connected end-to-end with code-style reliability calibration needed for design adoption [1–3,9–11].

This study proposes explainable boosting-based machine-learning (ML) surrogates for ETF web-crippling resistance

© 2026 The Author(s). ce/papers published by John Wiley & Sons Ltd.

This is an open access article under the terms of the Creative Commons Attribution-NonCommercial License, which permits use, distribution and reproduction in any medium, provided the original work is properly cited and is not used for commercial purposes

of sigma sections. The workflow combines (i) a validated FE database, (ii) boosted ensembles (e.g., gradient boosting, XGBoost, LightGBM and CatBoost) optimised by Bayesian search [5–8], (iii) transparent interpretation using SHAP [4], (iv) benchmarking against design equations [1–3, 10, 11], and (v) reliability calibration in the AISI S100 format to obtain design-ready resistance and safety factors [1].

2 Finite-Element Database and Validation

A nonlinear finite-element (FE) model was developed in ABAQUS to simulate ETF web crippling of sigma sections with intermediate stiffeners. The modelling strategy follows established practice for web-crippling simulation of thin-walled members: sigma sections were idealised using centreline shell elements with graded mesh density in corner regions, rigid bearing plates applied displacement-controlled loading, and surface-to-surface contact with friction governed load transfer. Quasi-static conditions were ensured using ABAQUS/Explicit by maintaining a low kinetic-to-internal energy ratio throughout the analysis [9–11].

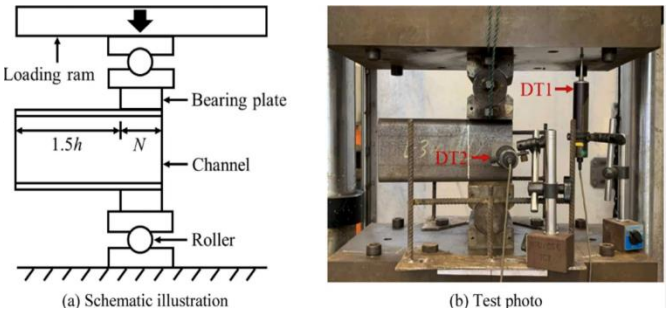


Figure 1. ETF loading test configuration (schematic) and definition of bearing length. Ensemble Modelling, Benchmarking and Reliability Framework.

1.01 and coefficients of variation below 5%, confirming the suitability of the FE framework for parametric studies [10, 11]. A subsequent parametric campaign produced 756 converged simulations spanning section geometry (depth D, thickness t, inside radius r, flange/lip and stiffener dimensions b_f, b_l, w_2, w_3), bearing length L_b, and yield strength f_y. Table 1 summarises the main variable ranges, while Figures 1–2 illustrate the ETF configuration and the overall modelling-to-ML workflow.

Table 1. Summary of key variables in the FE database (N = 756).

Feature	Mean	Min	Median	Max
D	220	140	220	300
t	1.83	1.00	2.00	2.50
r	5.00	3.00	5.00	7.00
L_{bl}	100.00	50.00	100.00	150.00
b_f	60.00	50.00	50.00	90.00
b_1	16.25	15.00	15.00	20.00
w_2	24.00	16.00	20.00	40.00
W_3	143.47	66.36	144.95	217.89
f_y	327.14	180.00	220.00	550.00
R_b	4.59	0.15	4.09	16.25

NB: Material type was encoded as 1=Aluminium, 2=Carbon steel, and 3=Stainless steel.

3 Methods: Boosted Ensembles, Benchmarking, SHAP and Reliability

Boosted tree ensembles were trained to map geometric and material descriptors to the FE reference capacity P_{uc}. The primary models are Gradient Boosted Regression Trees (GBRT) and modern boosting implementations (XGBoost, LightGBM and CatBoost), which are widely used for high-accuracy nonlinear regression with interaction effects [5–8]. Random Forest and AdaBoost were also trained as secondary baselines. Hyperparameters were tuned using Bayesian optimisation (Optuna) with cross-validation on the training set, and final performance was reported on a stratified held-out test set.

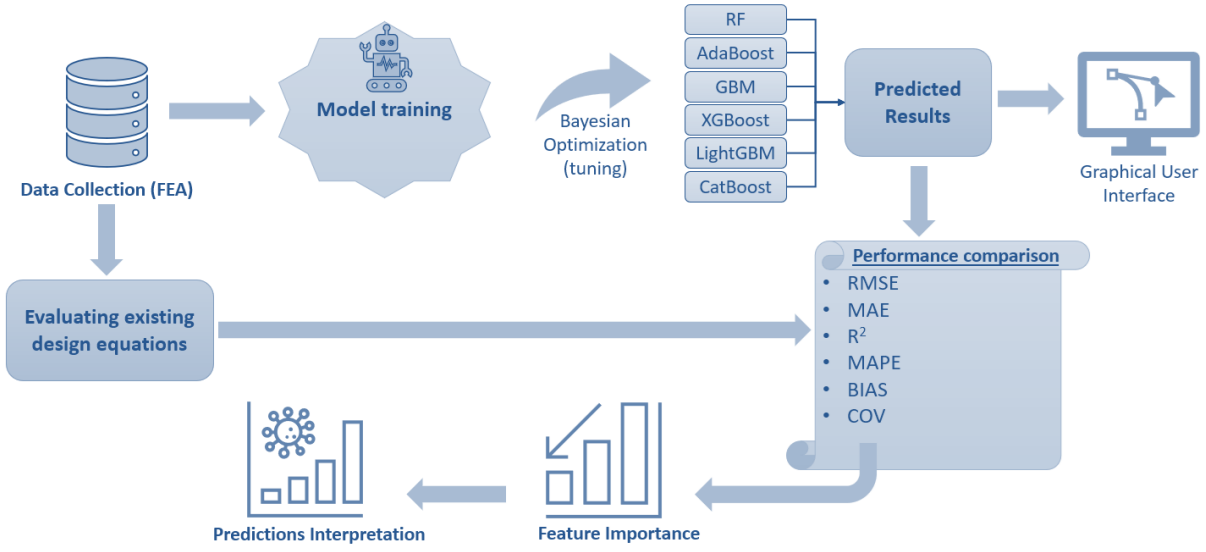


Figure 2. Workflow: FE database → boosted ensembles → SHAP interpretation → code benchmarking → reliability calibration

25097075, 2026, 2-3, Downloaded from https://onlinelibrary.wiley.com/doi/10.1002/cepa.70754 by Imperial College London, Wiley Online Library on [06/10/2026]. See the Terms and Conditions (https://onlinelibrary.wiley.com/terms-and-conditions) on Wiley Online Library for rules of use; OA articles are governed by the applicable Creative Commons License

Model accuracy is reported using R^2, RMSE and MAE (in kN). For benchmarking, the same dataset was evaluated using code-based and literature design equations for ETF web crippling, including AISI S100 / AS-NZS 4600, EN 1993-1-3, and AS/NZS 4673 (stainless steel), together with representative extensions and proposals by Husam et al., McIntosh et al., and Sundararajah et al. [1–3, 10, 11]. This enables a direct comparison between boosted-ensemble predictions and commonly used design formulations.

Interpretability is provided using SHAP (Shapley Additive ExPlanations), which decomposes each prediction into additive feature contributions expressed in engineering units and satisfies local accuracy and consistency properties [4]. Finally, a reliability calibration consistent with the AISI S100 format was performed using the model-error ratio $P = P_{uc}^{FE}/P_{uc}^{ML}$to compute LRFD resistance factors $\phi$and ASD safety factors $\Omega$from the bias and dispersion of P, adopting standard AISI calibration constants and minimum model-variability provisions [1].

4 Results and Discussion

4.1 Ensemble model accuracy

Table 2 summarises the test-set performance of the evaluated ensemble models. The boosting-based ensembles dominate: CatBoost and XGBoost achieve near-perfect agreement with the NLFEA targets ($R^2 = 1.000$), with RMSE of approximately 0.07–0.08 kN and MAE of about 0.05 kN. GBRT and LightGBM perform similarly well ($R^2 \approx 0.999$), with slightly higher but still very small errors (RMSE ≈ 0.09–0.10 kN; MAE ≈ 0.06–0.07 kN). In contrast, the bagging-based Random Forest shows markedly larger residuals, indicating reduced fidelity for this interaction-dominated, mixed-material response surface. Overall, the parity plots in Figure 3 confirm that the boosting models reproduce the FE response with minimal scatter across the full-strength range, consistent with the established capability of gradient-boosting algorithms for nonlinear regression in engineering datasets [5–8].

Table 2. Test-set accuracy of ensemble models for ETF web-crippling capacity prediction (metrics in kN)

Model	R² (test)	RMSE (kN)	MAE (kN)
Random Forest	0.974	0.573	0.399
AdaBoost	0.992	0.324	0.217
GBRT	0.999	0.095	0.065
LightGBM	0.999	0.099	0.066
CatBoost	1.000	0.071	0.049
XGBoost	1.000	0.076	0.051

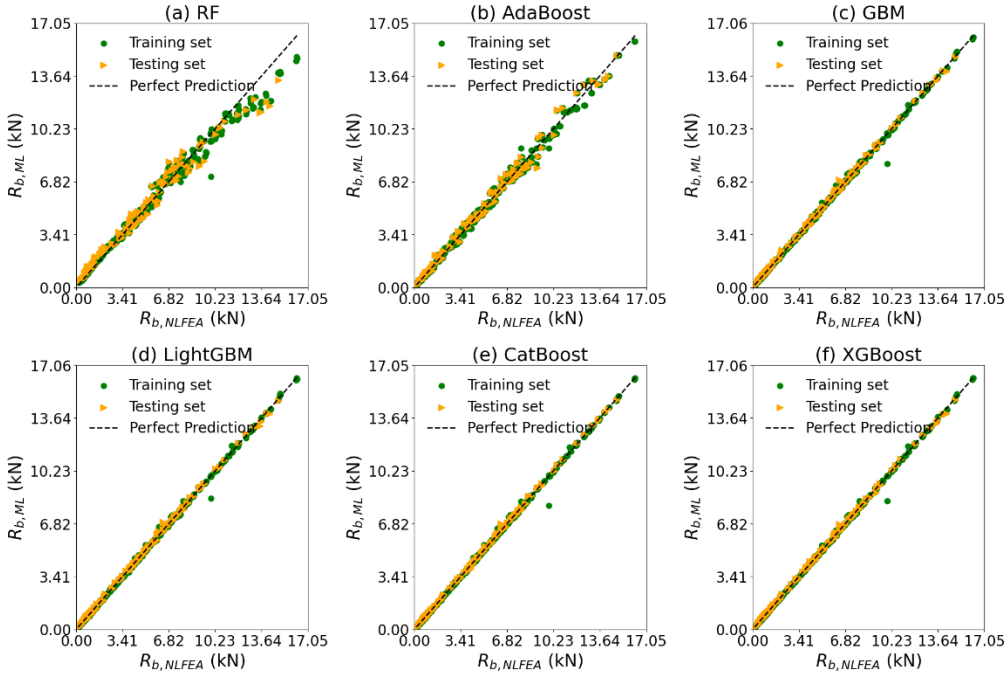


Figure 3 Parity plots for ensemble models (CatBoost/XGBoost/LightGBM/GBRT; RF and AdaBoost)

4.2 Comparison with design equations

Figure 4 shows that predictions from existing design equations show substantial scatter when applied to sigma sections with intermediate stiffeners. As summarised in Table 3, the mean ratio $P_{uc}^{FE}/P_{uc}^{pred}$ranges from 0.80 to 1.58, and the corresponding coefficients of variation reach or exceed 1.0 for several formulations. This behaviour reflects the sensitivity of ETF web crippling to coupled geometry–material interactions (e.g., stiffener restraint, bearing length effects and yield strength dependence) that are not fully captured by semi-empirical rules calibrated primarily on channel and Z-sections [1–3, 10, 11]. In contrast, the boosted ensemble models provide ratios close to unity

25097075, 2026, 2-3, Downloaded from https://onlinelibrary.wiley.com/doi/10.1002/cepa.70754 by Imperial College London, Wiley Online Library on [06/10/2026]. See the Terms and Conditions (https://onlinelibrary.wiley.com/terms-and-conditions) on Wiley Online Library for rules of use; OA articles are governed by the applicable Creative Commons License

with CoV ≤ 0.03, indicating near-unbiased predictions with very low dispersion, while retaining code-like computational efficiency.

Values of $P_{uc}^{FE}/P_{uc}^{pred} > 1.0$indicate conservative predictions (the equation underestimates capacity), whereas values <1.0indicate unconservative predictions (the equation overestimates capacity).

Table 3. Capacity-ratio statistics for design equations and best ML models (ETF, sigma sections).

	Rb (FE)/Rb(pred)	
Method	Mean	CoV
AISI S100 / AS-NZS 4600	0.95	0.58
Sundararajah et al.	0.80	2.37
EN 1993-1-3	1.36	1.10
Husam et al.	1.36	0.28
AS/NZS 4673	1.58	1.18
McIntosh et al.	0.88	2.18
CatBoost	1.00	0.02
XGBoost	1.00	0.03

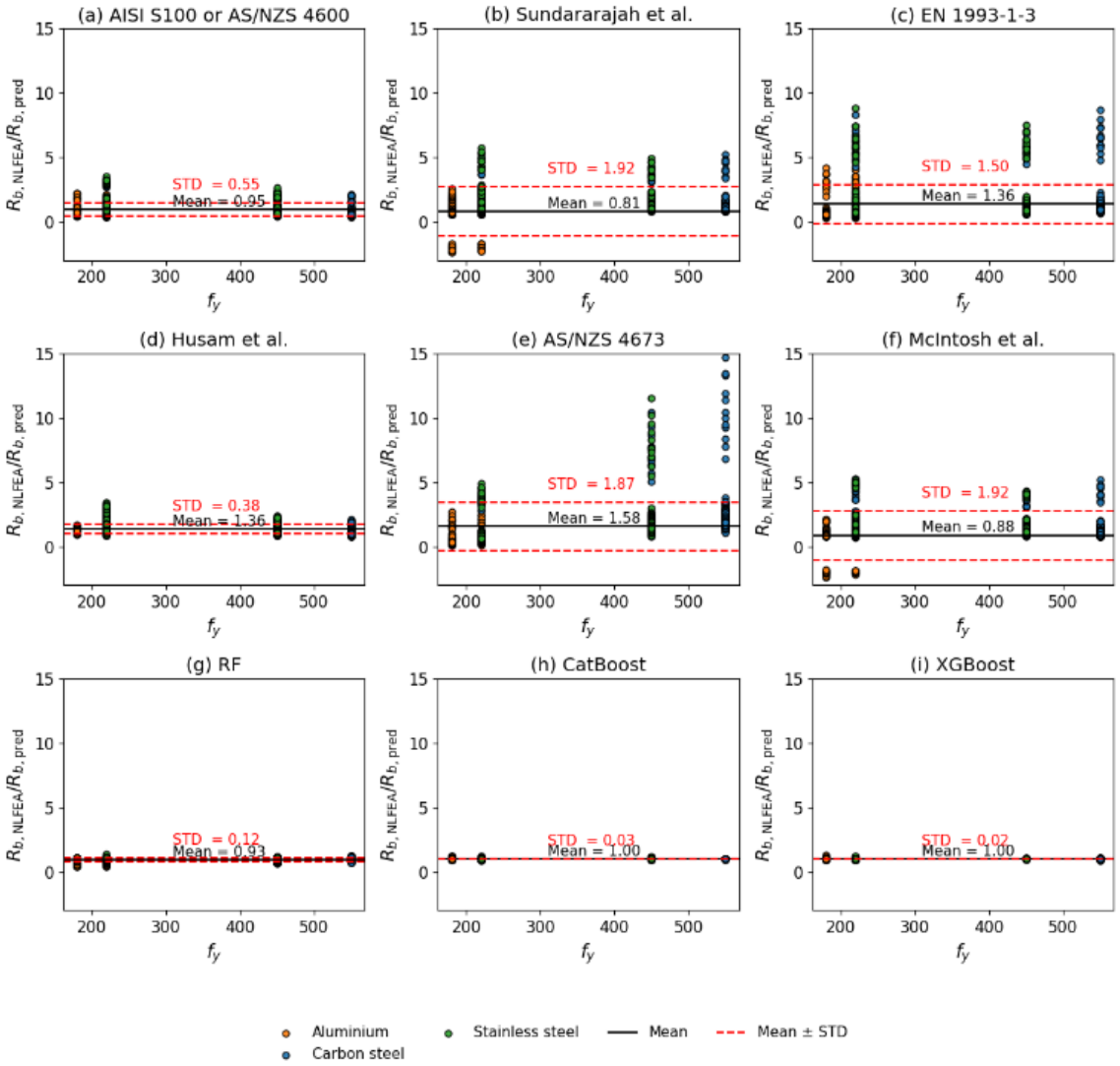


Figure 4. Normalised capacity ratio Rb(FE)/Rb(pred) versus fy for design equations and selected ML models.

4.3 SHAP interpretation and interaction effects

To interpret the best-performing boosted ensemble (CatBoost/XGBoost), SHapley Additive exPlanations (SHAP) were computed to decompose each prediction of web-crippling resistance into additive feature contributions expressed in engineering units, satisfying local accuracy and consistency [4]. The SHAP beeswarm plot (Figure 5) and the feature ranking confirm that web thickness $t$is the dominant contributor to ETF resistance, followed by yield strength $f_y$and bearing length L_b. Section depth $D$and the remaining geometric descriptors (e.g., b_f, b_l, w_2, $w_3$and r) provide secondary contributions by modifying local restraint and load diffusion. This hierarchy is consistent with established mechanics of two-flange web crippling and with prior studies highlighting thickness- and strength-controlled bearing resistance [9–11].

25097075, 2026, 2-3, Downloaded from https://onlinelibrary.wiley.com/doi/10.1002/cepa.70754 by Imperial College London, Wiley Online Library on [06/10/2026]. See the Terms and Conditions (https://onlinelibrary.wiley.com/terms-and-conditions) on Wiley Online Library for rules of use; OA articles are governed by the applicable Creative Commons License

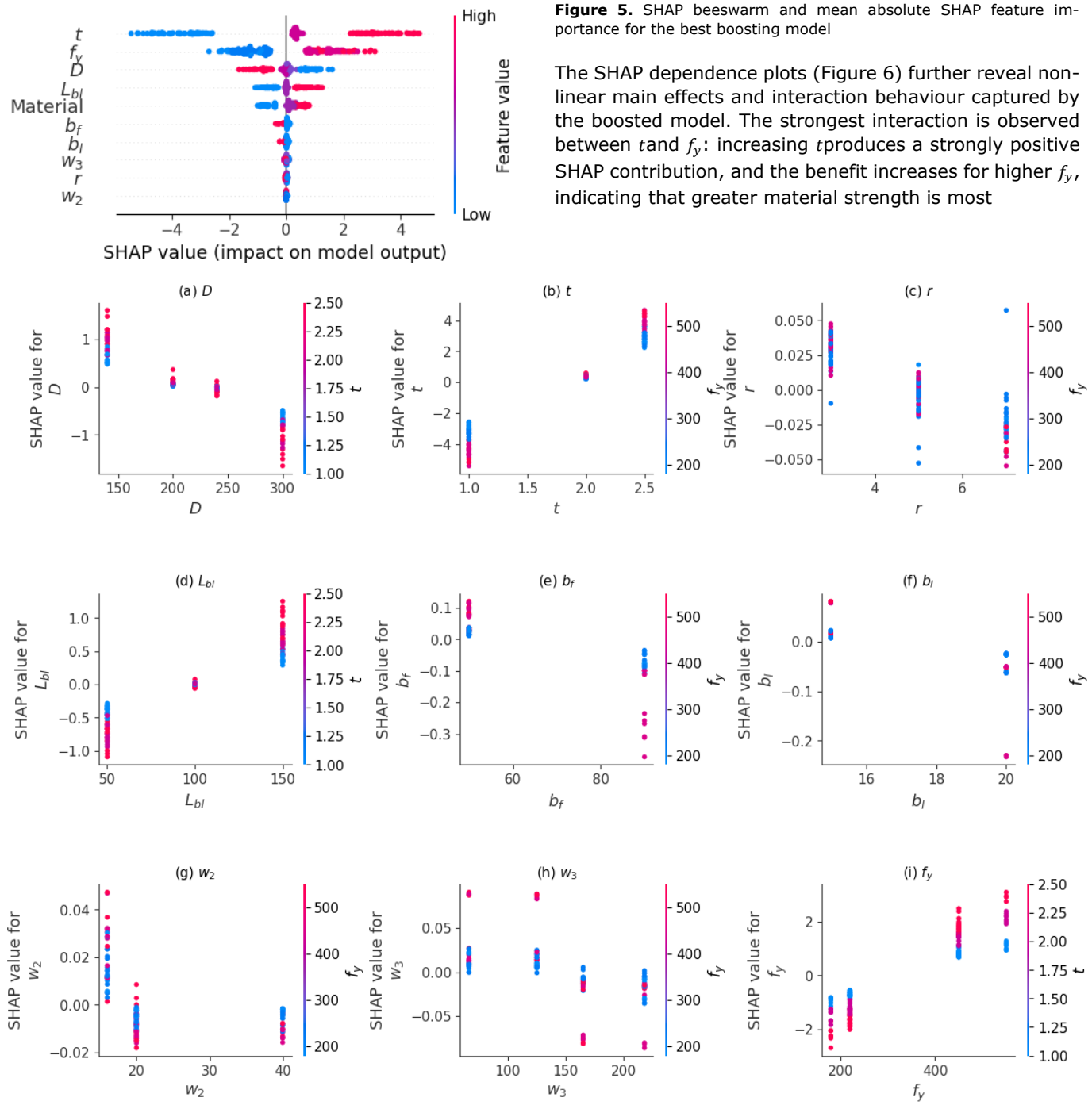


Figure 5. SHAP beeswarm and mean absolute SHAP feature importance for the best boosting model

Figure 5. SHAP dependence plots illustrating nonlinear main effects and interaction trends for the key inputs (D, t, r, L_b, b_f, b_l, w_2, w_3, f_y).

The SHAP dependence plots (Figure 6) further reveal nonlinear main effects and interaction behaviour captured by the boosted model. The strongest interaction is observed between $t$and f_y: increasing $t$produces a strongly positive SHAP contribution, and the benefit increases for higher f_y, indicating that greater material strength is most effectively mobilised when the web is sufficiently thick to delay local instability. A similar compensating interaction is evident between $L_b$and t: short bearing lengths yield negative contributions due to increased stress concentration, while larger $L_b$shifts SHAP values upward, and thicker webs partially offset the penalty associated with small L_b. These patterns are mechanically plausible because thickness increases local stiffness and reduces deformation beneath the bearing plate, while longer bearings improve load spreading and delay web yielding/buckling.

The influence of section depth $D$is generally unfavourable, with increasing Dtending to reduce predicted resistance, particularly for thinner webs (Figure 6a). This reflects the role of web slenderness and distortion effects in ETF loading, where larger web panels are more susceptible to local instability unless stabilised by sufficient thickness. For secondary geometry variables, the dependence plots indicate diminishing returns**:** stiffener dimensions $w_2$and $w_3$as well as flange/lip dimensions $b_f$and $b_l$contribute modestly and tend to plateau beyond thresholds where restraint is already effective. Overall, Figures 5–6 demonstrate that the boosted model captures physically meaningful interaction patterns—especially t–f_y synergy and L_b–t compensation—providing a transparent and mechanics-consistent basis for using ensemble surrogates in ETF web-crippling assessment [4, 5–8, 12].

4.4 Reliability-based design factors

Using the AISI S100 reliability format and the model-error statistics of the best boosting models, the calibrated LRFD resistance factors cluster around $\phi \approx 0.90$and ASD safety

25097075, 2026, 2-3, Downloaded from https://onlinelibrary.wiley.com/doi/10.1002/cepa.70754 by Imperial College London, Wiley Online Library on [06/10/2026]. See the Terms and Conditions (https://onlinelibrary.wiley.com/terms-and-conditions) on Wiley Online Library for rules of use; OA articles are governed by the applicable Creative Commons License

factors around $\Omega \approx 1.77–1.78$ (Table 4). The close agreement across models reflects their low dispersion and near-unbiased mean error, supporting practical adoption of boosted ensemble surrogates in ETF web-crippling design checks [1].

Table 4. Reliability calibration (AISI S100 format) for the best boosting models (ETF).

Model	ϕ (LRFD)	Ω (ASD)
CatBoost	0.90	1.77
XGBoost	0.90	1.77
Recommended (rounded)	0.90	1.78

4.5 Limitations and future work.

Although the proposed framework performed very well within the studied domain, some limitations should be noted. The model was trained on a finite-element database covering practical sigma-section geometries, so predictions for extreme or unconventional geometries may be less reliable. The study is also limited to ETF loading, and other cases such as eccentric, partial-bearing, uniform, or edge loading were not considered. In addition, the ML model depends on the fidelity of the underlying FE simulations, and any FE modelling assumptions may influence the predictions. Finally, while the trained model is computationally efficient in use, generating the FE database is computationally expensive. Future work should therefore extend validation to other loading cases and wider geometric ranges.

5 Conclusions

This study presented explainable boosted ensemble models for predicting the ETF web-crippling resistance of cold-formed steel sigma sections using a validated nonlinear FE database of 756 cases. The best models (CatBoost, XGBoost, LightGBM, and GBRT) achieved very high accuracy and clearly outperformed existing code-based equations, showing that boosted ensembles can serve as efficient and reliable surrogates for FE analysis. SHAP interpretation confirmed that web thickness, yield strength, and bearing length are the dominant drivers of resistance, with trends consistent with web-crippling mechanics. Reliability calibration within the AISI S100 framework further yielded stable design factors for the best models, with recommended values of $\phi \approx 0.90$ and $\Omega \approx 1.78$. Overall, the results support the use of interpretable ML surrogates for ETF web-crippling assessment of sigma sections and future refinement of design provisions.

6 References

[1] AISI (2016). *North American Specification for the Design of Cold-Formed Steel Structural Members*. AISI S100. American Iron and Steel Institute, Washington, DC, USA.

[2] CEN (2005). *EN 1993-1-3: Eurocode 3—Design of steel structures—Part 1-3: Cold-formed members and sheeting.* European Committee for Standardization, Brussels, Belgium.

[3] Standards Australia/Standards New Zealand (2018). *AS/NZS 4600: Cold-formed steel structures. Standards Australia/Standards New Zealand*, Sydney/Wellington.

[4] Lundberg, S.M., Lee, S.-I. (2017). *A unified approach to interpreting model predictions.* Advances in Neural Information Processing Systems (NeurIPS).

[5] Friedman, J.H. (2001). *Greedy function approximation: A gradient boosting machine*. Annals of Statistics, 29(5), 1189–1232.

[6] Chen, T., Guestrin, C. (2016). *XGBoost: A scalable tree boosting system*. In: Proceedings of the 22nd ACM SIGKDD International Conference on Knowledge Discovery and Data Mining (KDD), 785–794.

[7] Ke, G., et al. (2017). *LightGBM: A highly efficient gradient boosting decision tree*. In: Advances in Neural Information Processing Systems (NeurIPS).

[8] Prokhorenkova, L., et al. (2018). *CatBoost: Unbiased boosting with categorical features.* In: Advances in Neural Information Processing Systems (NeurIPS).

[9] Thirunavukkarasu, K., et al. (2024). *Web crippling behaviour of sigma sections under end-two-flange loading—Numerical investigation.* Structures, 59, 105765.

[10] Sundararajah, L., et al. (2017). *New design rules for lipped channel beams subject to web crippling under two-flange load cases.* Thin-Walled Structures, 119, 421–437.

[11] McIntosh, A., et al. (2021). *Web crippling of cold-formed carbon steel, stainless steel and aluminium channels: Investigation and design*. Journal of Constructional Steel Research, 179.

[12] Simwanda, L., et al. (2024). *Explainable machine learning models for predicting the ultimate bending capacity of slotted perforated cold-formed steel beams under distortional buckling.* Thin-Walled Structures, 205, 112587.

25097075, 2026, 2-3, Downloaded from https://onlinelibrary.wiley.com/doi/10.1002/cepa.70754 by Imperial College London, Wiley Online Library on [06/10/2026]. See the Terms and Conditions (https://onlinelibrary.wiley.com/terms-and-conditions) on Wiley Online Library for rules of use; OA articles are governed by the applicable Creative Commons License